

Noise effect on 2D photoluminescence decay analysis using the RATS method in single-pixel camera configuration

JIRÍ JUNEK,^{1,2,*} KAREL ŽÍDEK,¹

¹Regional Center for Special Optics and Optoelectronic Systems (TOPTEC), Institute of Plasma Physics, Czech Academy of Science v.v.i., Za Slovankou 1782/3, 182 00 Prague 8, Czech Republic

²Technical University in Liberec, Faculty of Mechatronics, Informatics and Interdisciplinary Studies, Studentská 1402/2, 461 17 Liberec, Czech Republic

*junekj@ipp.cas.cz

Abstract: Using a random temporal signal for sample excitation (RATS method) is a new, efficient approach to measuring photoluminescence (PL) dynamics. The method can be used in single-point measurement (0D), but also it can be converted to PL decay imaging (2D) using a single-pixel camera configuration. In both cases, the reconstruction of the PL decay and PL snapshot is affected by ubiquitous noise. This article provides a detailed analysis of the noise effect on the RATS method and possible strategies for its elimination. We carried out an extensive set of simulations focusing on the effect of noise introduced through the random excitation signal and the corresponding PL waveform. We show that the PL signal noise level is critical for the method. Furthermore, we analyze the role of acquisition time, where we demonstrate the need for a non-periodic excitation signal. We show that it is beneficial to increase the acquisition time while increasing the number of measurements in the single-pixel camera configuration has a minimal effect above a certain threshold. Finally, we study the effect of a regularization parameter used in the deconvolution step, and we observe that there is an optimum value set by the noise present in the PL dataset. Our results provide a guideline for optimization of the RATS measurement, but also study effects generally occurring in PL decay measurements methods relying on the deconvolution step.

© 2021 Optica Publishing Group under the terms of the [Optica Publishing Group Open Access Publishing Agreement](#)

1. Introduction

Fluorescence lifetime imaging (FLIM) is a frequent spectrometric analysis in biology [1,2], chemistry [3], and materials engineering [4]. There are various techniques for measuring or evaluating PL dynamics like time-correlated single photon counting [5], gated PL counting [6], streak camera [7], time-domain or frequency-domain analog recording technique [8,9]. Another available method for PL decay measurement is based on random excitation of the measured sample - the RATS method [10], which could also be set in single-pixel camera (SPC) configuration [11] and carry out the FLIM experiment. We abbreviate this measurement as 2D-RATS.

The 2D-RATS method combines the SPC technique with the excitation of the PL with random patterns (masks) blinking randomly in time. Each mask leads to a specific PL decay, which is measured for a set of uncorrelated masks. Then, using algorithms for undetermined systems, it is possible to reconstruct PL decays in each individual pixel of the 2D scene. The quality of reconstruction is affected by noise, which is inevitably present in all measured data. Therefore, the noise analysis of the method is an essential piece of knowledge that allows optimization of the method and identifies the most sensitive aspects of the setup. Moreover, many results valid for the RATS method are also relevant for the PL measurement, where the deconvolution step is used [12].

In this article, we carry out a detailed study of various noise effects on the 2D-RATS measurement and their impact on the resulting FLIM information. Our analysis is based on extensive simulations and a set of synthetic data faithfully following the real experimental conditions for the SPC experiment carried with a digital micro-mirror device. We analyze the benefits of various approaches to noise reduction. Besides the generally used option to prolong the acquisition time [13], the deconvolution step in the RATS method allows us to optimize the regularization parameter of the deconvolution [14,15]. Due to the random nature of the excitation signal in RATS, we avoid the use of any mathematical filters which can be apparently optimized for one type of signal, but due to the possibility of choosing a different signal frequency and sampling, such a filter can be difficult to transfer to a general case.

Our article provides guidelines for optimizing experiments for PL decay measurement and FLIM, where the deconvolution-based retrieval of PL dynamics is used. We demonstrate that the noise present in the PL dataset is the most critical factor. At the same time, we show that the resulting noise level in the FLIM dataset can be highly decreased by using a longer non-periodic excitation signal or by optimizing the regularization parameter. The parameter features an optimum value for a given noise level. We point out the issues connected to a periodic excitation signal.

In particular, we demonstrate that with proper choice of regularization parameter and acquisition time, the RATS method can attain results that are not distorted at all and can accurately map a 2D scene even with a relatively high noise level (3%).

2. RATS method

We will first introduce the principles of the single-spot 0D-RATS method and imaging 2D-RATS measurement. The cornerstone of the RATS method is sample excitation with a random signal I_{EXC} . PL signal I_{PL} is a convolution of I_{EXC} and PL decay I_D (Eq.(1)).

$$I_{PL} = I_{EXC} * I_D. \quad (1)$$

This fact can be used to recover the PL decay from I_{PL} by using the Fourier transform and the convolution theorem. The deconvolution is attainable only for the frequencies where the excitation signal has a non-zero amplitude. Nevertheless, due to random excitation, a single measurement contains a broad range of frequencies in a single dataset. PL decay I_D could then be determined via deconvolution (Eq.(2)).

$$I_D = Re \left\{ \mathbb{F}^{-1} \left[\frac{\mathbb{F}(I_{PL}) \mathbb{F}^*(I_{EXC})}{\mathbb{F}(I_{EXC}) \mathbb{F}^*(I_{EXC}) + \varepsilon \mathbb{F}(I_{EXC}) \mathbb{F}^*(I_{EXC})} \right] \right\}. \quad (2)$$

The 2D-RATS measurement is carried out in an SPC configuration, as we described in our previous article [11]. We point the reader to numerous articles summarizing the SPC experiment for more details [16-19]. In our implementation of the SPC experiment, the sample was illuminated with a set of random excitation patterns (masks). The excitation masks were "blinking" with the same waveform $I_{EXC}(t)$, and the whole PL from each illuminated point i is collected to a single-pixel detector. Hence, the photoluminescence I_{PL} is given as a summation of $I_{PL}(i)$ signals. Then Eq.(1) can be rewritten for the total PL intensity as:

$$I_{PL} = \sum_{i=1}^n I_{PL}(i) = I_{EXC} * \sum_{i=1}^n I_D(i). \quad (3)$$

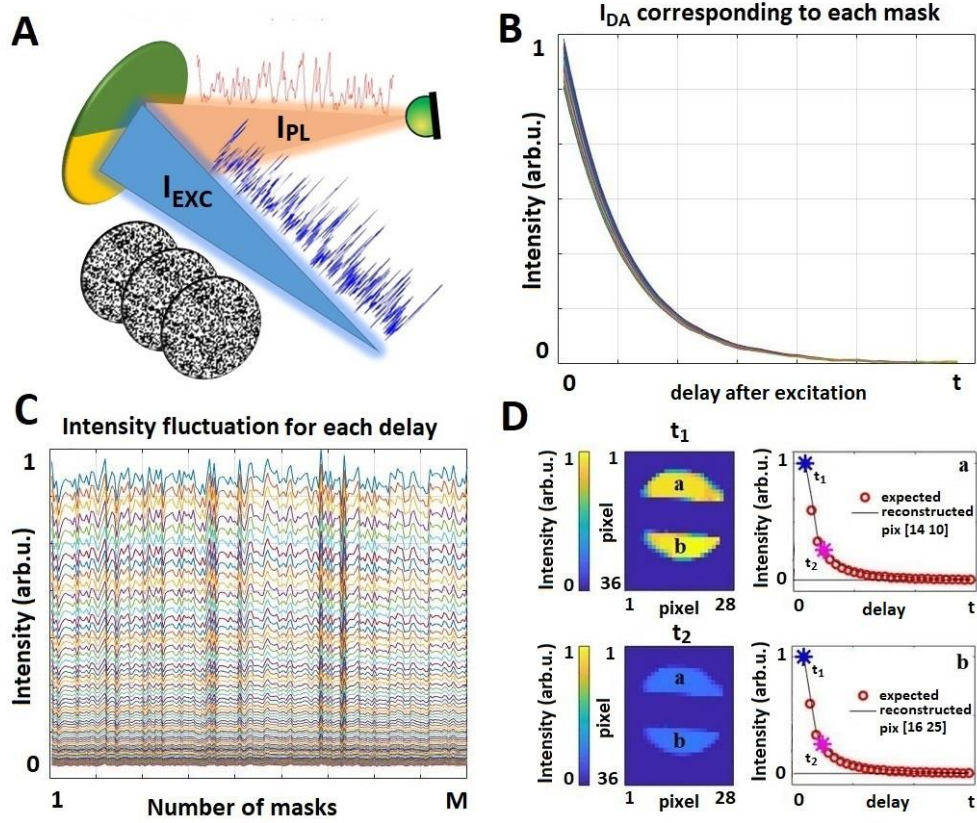


Figure 1: (A) Scheme of 2D-RATS approach, where the sample is illuminated with a set of random patterns (masks) blinking according to I_{EXC} . The total PL intensity waveform I_{PL} is detected for each mask with a single-pixel detector. (B) Example of a set of calculated I_{DA} 's for corresponding masks – see Eq.(4). (C) Intensity fluctuation for each delay after excitation of I_{DA} . Knowing the fluctuation (I_{SPC} signal) and set of masks makes it possible to determine the PL map m at a given delay after excitation of I_{DA} using compressed sensing algorithms. (D) An example of reconstructed PL maps in delays t_1 and t_2 . Plotted I_D 's corresponding to pixel [14 10] (area "a") and to pixel [16 25] (area "b").

The number of excitation masks M is set by the number of image pixels N and the so-called compression ratio $k = M/N$. Because masks are not coherent, i.e., one pattern is not correlated with each other, each mask illuminates a different combination of the sample pixels, and, therefore, each mask represents its own I_{PL} , which can be used to retrieve the PL decay I_{DA} :

$$I_{DA} = Re \left\{ \mathbb{F}^{-1} \left[\frac{\mathbb{F} \left(\sum_{i=1}^n I_{PL(i)} \right) \mathbb{F}^* (I_{Exc})}{\mathbb{F} (I_{Exc}) \mathbb{F}^* (I_{Exc}) + \epsilon \mathbb{F} (I_{Exc}) \mathbb{F}^* (I_{Exc})} \right] \right\}. \quad (4)$$

PL snapshot $m(t)$ can be reconstructed in each delay after excitation t using the calculated $I_{DA}(t)$ curves. For the given delay and each excitation mask, the $I_{DA}(t)$ provides a dataset I_{SPC} describing intensity fluctuation of M values – see Fig. 1(C), where each curve corresponds to a single I_{SPC} dataset. Then PL snapshot $m(t)$ is then retrieved from the underdetermined dataset by using a standard SPC retrieval:

$$\min\{\|Am(t) - I_{SPC}\|_2^2 + TV(m(t))\}. \quad (5)$$

The sensing matrix A is formed from vectorized excitation patterns, TV stands for the total variation calculation.

By reconstructing a temporal snapshot for each delay t , we get a 3D datacube, which contains PL decay in every i -th pixel of the sample $I_D(i, t)$. The whole concept is illustrated and summarized in Fig. 1.

3. Noise effect simulation

A small contribution of noise can be expected in each measured signal in the experiment. In order to maintain stable conditions, the role of the noise was explored through simulations. A primary signal I_{EXC} was simulated using temporal speckles patterns [20], which are cornerstones of a random analog signal generator presented in our previous work [10]. The length of the simulated I_{EXC} signal was 0.1 s with an impulse response function of FWHM of $2.07\mu\text{s}$. The PL decay I_D was considered with the lifetime $\tau = 20\mu\text{s}$. Used noise levels throughout the article are consistent with the noise that can be expected in a realistic experiment [12]. The excitation signal I_{EXC} was simulated as non-periodic. The importance of a non-periodic signal will be explained in section 4.1. It is worth noting that with the exception of section 4.3, the regularization parameter ε (Eq.(2) and Eq.(4), respectively) is considered as $\varepsilon = 0.1$.

3.1 0D-RATS

To demonstrate the basic steps, we shall start with the non-imaging RATS, i.e., 0D-RATS. We use two datasets of I_{EXC} and I_{PL} , which are subsequently used to retrieve the PL decay via Eq.(2). Therefore, we initially simulated the effect of noise present in these two datasets.

Firstly, we added white noise to I_{EXC} , while I_{PL} was kept absolutely noiseless (Fig. 2(A)) and vice versa (Fig. 2(B)). In both datasets in Fig. 2, the signal-to-noise ratio (SNR) was 15.2 dB which corresponds to 3% percent of noise in the system (see Eq.(6)).

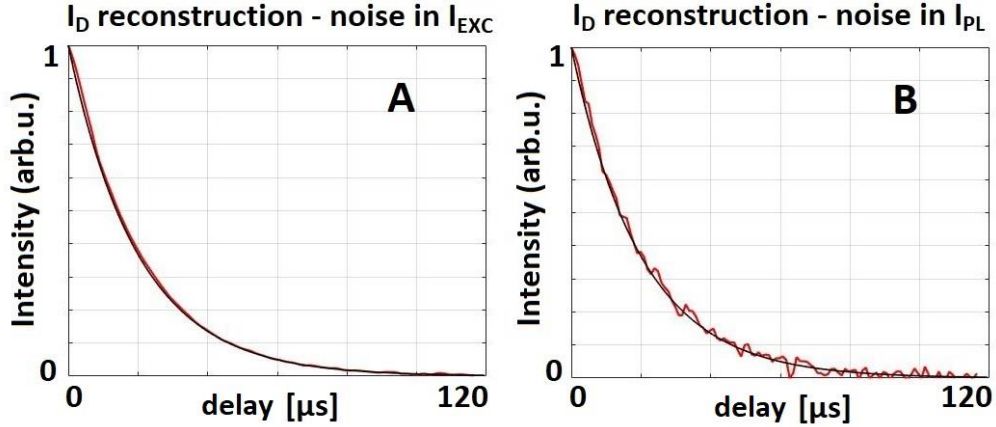


Fig 2: (A) Reconstructed I_D with a noise level of 3% in I_{EXC} , which corresponds with SNR about 15.2 dB. I_{PL} was assumed noiseless. (B) Reconstructed I_D with a noise level of 3% in I_{PL} , corresponding with SNR about 15.2 dB. I_{EXC} was assumed noiseless.

$$SNR[dB] = -10 \log_{10} \left(\frac{\text{noise}[\%]}{100} \right). \quad (6)$$

For both retrieved decays in Fig. 2 (red lines), the noise had an effect on reconstructed I_D , but the measured PL dynamics were not biased, i.e., the overall decay shape was not altered,

and it was in perfect agreement with the expected output (black lines). Nevertheless, we observed that the noise in the I_{PL} dataset had a significantly more pronounced effect on the resulting noise in the retrieved PL decay (Fig. 2(B)).

We can quantify the noise level by the root-mean-square error, which reaches $RMSE_{PL} = 12,9 \cdot 10^{-3}$ for the noise in the PL signal and $RMSE_{EXC} = 2,8 \cdot 10^{-3}$ for the noise in the excitation signal. That suggests that regularization in the denominator of Eq.(2) has a more pronounced effect on I_{EXC} than I_{PL} , which becomes the dominating source of noise in the retrieved decay.

3.2 2D-RATS

As the next step, we also simulated the effect of noise in the I_{PL} and I_{EXC} signal on the 2D-RATS experiment. Here, the situation is more complex because the noise present in the I_{PL} and I_{EXC} datasets is first transposed into the noise of the retrieved PL decay curve $I_{DA}(t)$ from Eq.(4). The noise present in these curves is then propagating into the SPC signal I_{SPC} , which is then used for the retrieval of the set of PL snapshots for each delay in Eq.(5).

All simulated reconstructions were performed using binary masks. We used the reconstruction algorithm based on the sparsity of total variance TVAL3 [21,22]. The main parameters of the TVAL3 algorithm were: μ (2^{11}), β (2^7). As a measured sample, we used Matlab predefined image Phantom, where the PL decay with a single lifetime of $\tau = 20 \mu s$ was set to be constant all over the Phantom's "body". Acquisition time and other conditions simulating real experiments were kept the same as for the 0D-RATS simulations above.

We carried out the same calculation as we presented in Section 3.1, and we show in Fig. 3 the retrieved PL snapshots $m(t)$ in the peak PL intensity, i.e., $t = 0 \mu s$, where the contrast of the PL signal is the highest. The case was studied for three different SPC compression ratios $k = 0.4, 0.6, 0.8$ and four signal-to-noise ratios $SNR = 15.2, 18.2, 20, 23$ dB, which corresponds to 3%, 1.5%, 1%, 0.5% level of noise in the signal.

The results are summarized in Fig. 3 for the noise introduced in the I_{EXC} signal (left-hand side) and the noise introduced in the I_{PL} signal (right-hand side), and the corresponding resulting noise levels are presented in Table 1.

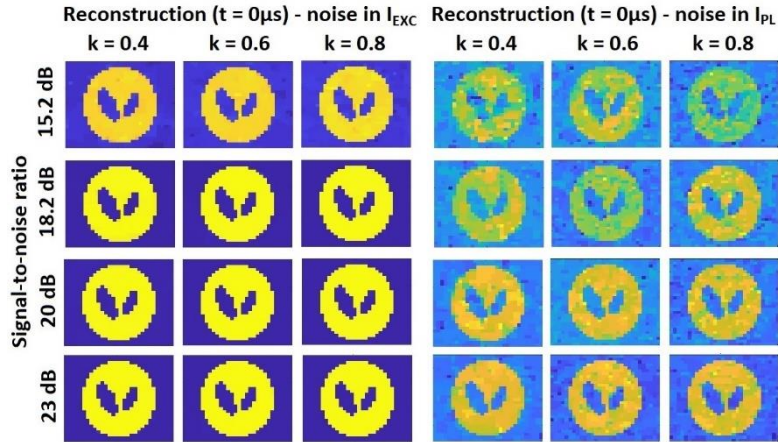


Figure 3: Left part: reconstructions of PL map m in delay with maximal intensity ($t = 0 \mu s$) in case of noise in I_{EXC} . Right part: reconstructions of PL map m in delay with maximal intensity ($t = 0 \mu s$) in case of noise in the I_{PL} . The noise parameters are for both $SNR = 15.2, 18.2, 20, 25$ dB (rows) and the compression ratios are $k = 0.4, 0.6, 0.8$ (columns).

Analogously to the 0D-RATS, the noise in I_{PL} has a significantly worse effect on the image retrieval than the noise in the I_{EXC} signal. By comparing different noise levels (compare lines in Fig. 3), one can see that the SNR of the I_{PL} is the main limiting factor in the snapshot retrieval. The effect of compression ratio (compare columns in Fig. 3) does not play any significant role

for the values above 0.4. This means that it is not efficient to compensate for higher noise in the measured signal by simply increasing the number of measured excitation masks.

To quantify the effect of each parameter, we introduced three different measures. Firstly, we can judge the image reconstruction quality, where we compare the retrieved snapshot m (in delay $t = 0 \mu\text{s}$) with the actual image used in simulations U by using Frobenius norm of the two:

$$R = \frac{\|m - U\|_F}{\|U\|_F}. \quad (7)$$

We can also focus on the PL dynamics for each pixel i , where the reconstructed decay curve $I_{DREC}(i)$ is normalized and compared with the actual decay curve $I_D(i)$, which was used to simulate the data. The comparison was made from $t_0 = 0 \mu\text{s}$ to $t_\tau = 120 \mu\text{s}$, which is a sufficient temporal range for the decay curve with a lifetime of $20 \mu\text{s}$. We denote this error as the decay deviation σ :

$$\sigma = \frac{1}{N} \sum_{i=1}^N \sum_{t=t_0}^{t_\tau} \sqrt{(I_{DREC}(i,t) - I_D(i,t))^2}. \quad (8)$$

Finally, we also determined the SNR of the I_{SPC} signal, which is used for the image retrieval m in delay $t = 0 \mu\text{s}$. Note that the I_{SPC} signal indicates the fluctuation of I_{DA} curves corresponding to the respective delay. The fluctuations (I_{SPC}) are affected by the noise in both I_{EXC} and I_{PL} . We extract the I_{SPC} noise level to provide a comparison to other SPC experiments. $SPC-SNR_{EXC}$ denotes the noise level in I_{SPC} when the noise was added to I_{EXC} and $SPC-SNR_{PL}$ indicates the case when the noise was added to the I_{PL} . Analogously, the indices "PL" and "EXC" have the same meanings for R_{EXC} and R_{PL} or σ_{EXC} and σ_{PL} .

Table 1: Quality of the retrieved image (R , lower number = higher quality) and SPC signal (SPC-SNR, higher number = higher quality) corresponding to Fig. 3 for noise introduced via I_{EXC} and I_{PL} signal.

	noise source	k	noise level			
			SNR 15.2dB	SNR 18.2dB	SNR 20dB	SNR 23dB
R	EXC	0.4	0.177	0.158	0.150	0.142
		0.6	0.175	0.155	0.149	0.142
		0.8	0.175	0.155	0.149	0.142
	PL	0.4	0.328	0.265	0.242	0.191
		0.6	0.312	0.264	0.215	0.192
		0.8	0.326	0.261	0.224	0.181
SPC-SNR	EXC	0.4	38.01	43.80	48.14	54.97
		0.6	38.06	43.84	48.05	55.04
		0.8	37.98	43.90	48.25	55.16
	PL	0.4	34.67	37.52	39.53	43.24
		0.6	34.86	37.45	40.01	43.10
		0.8	34.84	37.83	39.48	42.72

4. Noise level optimization

In Section 3, we studied the effect of the noise level in the I_{EXC}/I_{PL} simulated dataset on the retrieval of the PL decay curve and PL snapshot. The noise levels are determined by the properties of an optical setup, which features a certain photon budget (number of detectable

photons), types of detectors, and samples. For an optimized optical setup, such characteristics can not be easily improved.

On the other hand, it is possible to enhance the quality of the retrieved PL decay or FLIM on the expenses of the acquisition time. Therefore, we studied the benefits connected to a longer acquisition time. Due to the fact that the RATS method is based on signal deconvolution, an important factor is the periodicity of the signal, as we discuss in the following subsection.

4.1 Periodic extension of acquisition time

A straightforward approach to improve the quality of the PL decay I_D retrieval via Eq.(2) is to repeat the same measurement for the same excitation waveform. Hence, we attain a periodic I_{EXC} and I_{PL} signal. However, it is worth stressing that the use of a periodic signal I_{EXC} will create unwanted artefacts in the retrieved data. It follows from the nature of deconvolution in Eq.(2) that such periodic excitation waveform leads to a periodic I_D signal with a lower amplitude. We will demonstrate this effect on a 0D-RATS simulation.

We compare in Fig. 4 the entire retrieved PL decay (I_D curve) in the case of a non-periodic I_{EXC} signal with a length of 0.1 s (left-hand side) and a periodic I_{EXC} signal (7 periods) with the same total duration of 0.1 s. Their comparison shows that the amplitude of the retrieved PL for the periodic I_{EXC} signal is about seven times smaller compared to the non-periodic case and the PL signal has multiple replicas.

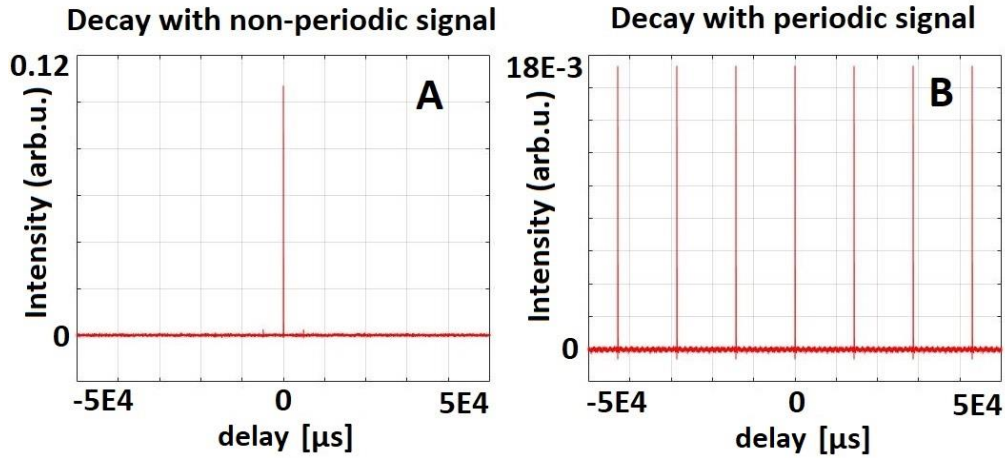


Figure 4: Results of I_D reconstruction (deconvolution), when non-periodic (panel A) and periodic (panel B) I_{EXC} was used for sample excitation with lifetime $\tau = 20 \mu\text{s}$.

When we zoom in Fig. 4(B) into the PL dynamics during the first hundreds of microseconds, i.e., one of the PL decay replicas, we get after normalization the correct I_D following the actual decay – see Fig. 5. However, the resulting SNR is decreased. We tested in Fig. 5 the noise introduced via the excitation signal I_{EXC} (panel A) and PL signal I_{PL} (panel B). The root-mean-square error for curves in Fig. 5 reaches $RMSE_{PL} = 29,7 \cdot 10^{-3}$ and $RMSE_{EXC} = 7,8 \cdot 10^{-3}$ for the noise introduced in the I_{PL} and I_{EXC} signal, respectively. The noise level in Fig. 5 can be directly compared to Fig. 2, where we used a non-periodic signal and where $RMSE_{PL} = 12,9 \cdot 10^{-3}$ and $RMSE_{EXC} = 2,8 \cdot 10^{-3}$. For the non-periodic signal, the resulting noise level was more than 2-times lower.

To further illustrate this behavior, we carried out a set of simulations, where we kept a constant total acquisition time of 0.1 s, while the I_{EXC} signal was set to be periodic with up to 16 periods – see Fig. 6. The root-mean-square error increases with the number of periods for both situations – noise in the I_{EXC} and I_{PL} signal. Therefore, for the sake of optimum signal reconstruction in the RATS method, it is worth avoiding any periodicity in the I_{EXC} signal.

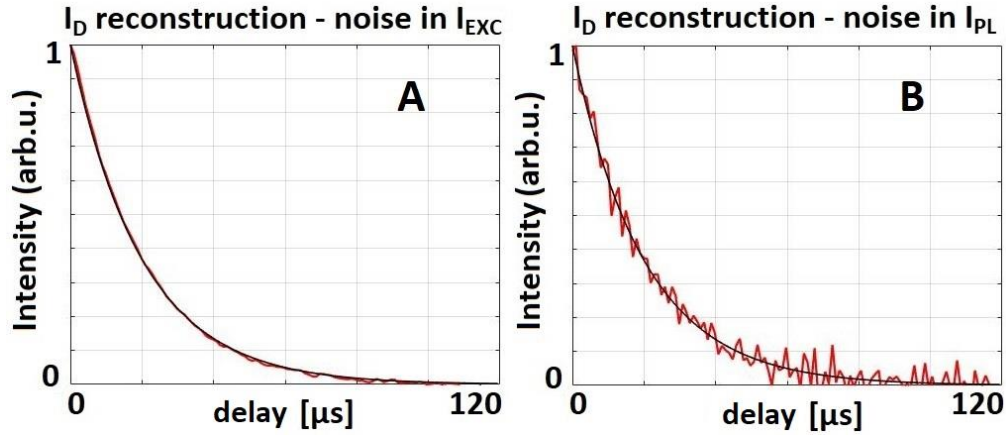


Figure 5: Zoomed results of I_D reconstruction ($\tau = 20 \mu\text{s}$), when I_{EXC} was used as a periodic signal (7 periods). Redline is reconstructed data, and the black line is reference data. (A) Reconstruction with an amount of noise of 3% in I_{EXC} (correspond with SNR about 15.2 dB). (B) Reconstruction with an amount of noise of 3% in I_{PL} (correspond with SNR about 15.2 dB).

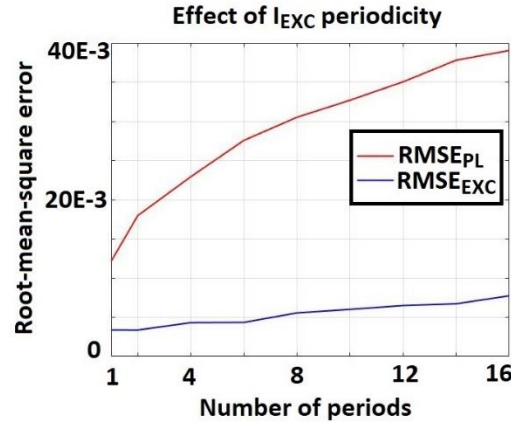


Figure 6: RMSE of I_D for a periodical I_{EXC} with a constant total acquisition time of $t_{acq} = 0.1 \text{ s}$. The number of periods in the I_{EXC} signal is varied. I_{PL}/I_{EXC} noise level: SNR 15.2 dB.

4.2 Non-periodic acquisition time extension

The possible way to eliminate the noise effect is to extend the acquisition time so that we avoid any I_{EXC} signal periodicity. This approach favors frequencies representing the true signal in the Fourier spectrum and suppresses the contribution of white noise. We carried out simulations corresponding to the 2D-RATS measurement presented in Fig. 3. Nevertheless, here we used a set of acquisition times $t_{acq} = 0.1 \text{ s}$, $t_{acq} = 0.2 \text{ s}$, $t_{acq} = 0.4 \text{ s}$, $t_{acq} = 1 \text{ s}$ and $t_{acq} = 2 \text{ s}$. Other conditions, such as reconstruction parameters, regularization parameter ε and signal properties, were kept the same as in Section 3.

As in Section 3.2, we focus on the quality of the retrieved image (R_{EXC} , R_{PL}), noise introduced into the SPC signal ($SPC-SNR_{EXC}$, $SPC-SNR_{PL}$) in delay $t = 0 \mu\text{s}$. Moreover, this section also focuses on the deviation of the whole reconstructed PL decay in each pixel of the sample (σ_{EXC} , σ_{PL}).

Dependences of each noise characteristics on the acquisition time are presented in Fig. 7-9. In these figure, the line/symbol color indicates the given SNR (red: 15.2dB, blue: 18.2dB, black: 20dB and magenta: 23dB); line/symbol type represent the compression ratio k (cross: 0.8, circle: 0.6, full line: 0.4).

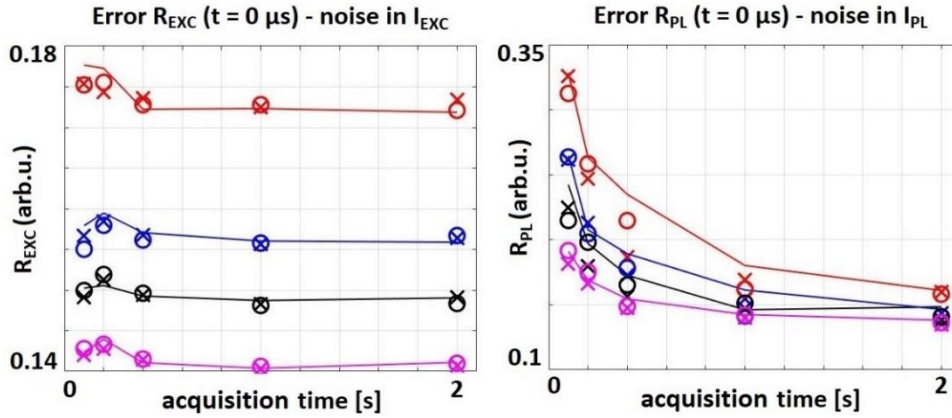


Figure 7: Reconstruction error R_{EXC} (left part), R_{PL} (right part) at the delay $t = 0 \mu s$ dependence on sensing time for different SNR: 15.2 dB (red), 18.2 dB (blue), 20 dB (black), 23 dB (magenta) and three different compression ratio $k = 0.4$ (full line), $k = 0.6$ (circle), $k = 0.8$ (cross).

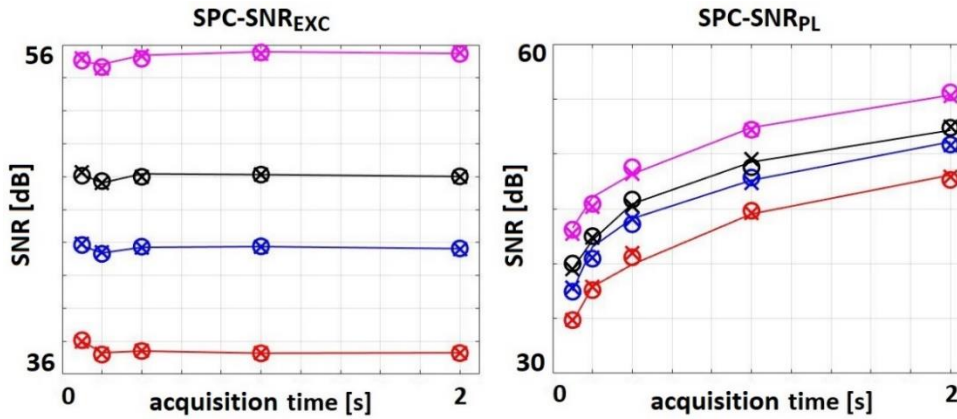


Figure 8: Noise dependence in SPC signal (random fluctuation in intensity of I_D in delay $t = 0 \mu s$, because of changing illumination masks) on sensing time according to added noise to I_{EXC} (left part) and I_{PL} (right part) with SNR: 15.2 dB (red), 18.2 dB (blue), 20 dB (black), 23 dB (magenta) and three different compression ratio $k = 0.4$ (full line), $k = 0.6$ (circle), $k = 0.8$ (cross).

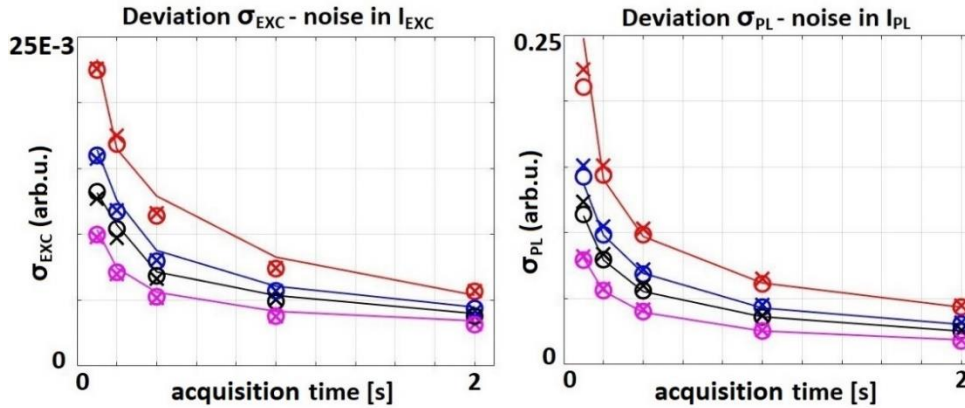


Figure 9: Acquisition time dependence of σ_{EXC} - noise added to I_{EXC} (left part) and σ_{PL} - noise added to I_{PL} (right part). SNR: 15.2 dB (red), 18.2 dB (blue), 20 dB (black), 23 dB (magenta) and three different compression ratio $k = 0.4$ (full line), $k = 0.6$ (circle), $k = 0.8$ (cross).

All the results in Fig. 7-9 confirm that the effect of noise level (varying color) is much more pronounced than the compression ratio (varying line/symbol type), i.e., increasing the number of excitation patterns above 40% compared to the number of the pixel has a negligible effect on the image quality.

When we focus on the noise introduced via I_{EXC} signal, it has a low effect on the resulting image reconstruction – see Fig. 3, left-hand side. For this reason, the change in the acquisition time has almost no effect on the resulting noise level regarding the image quality and SPC signal error (see Fig. 7-8).

On the contrary, for the noise introduced via the I_{PL} signal, we can highly improve the quality of the retrieved image by the increased acquisition time. This image quality enhancement is much more pronounced for higher noise levels. In the case where the noise level is 15.2 dB (3%), the R_{PL} will decrease by 50%, while when the noise level is 23 dB (0.5%), the R_{PL} will decrease by only 25%.

The results described in Fig. 7 are linked to the results presented in Fig. 8. As expected, the highest $SPC-SNR_{EXC}$ and $SPC-SNR_{PL}$ are reached for the lowest noise level in the system - $SNR = 23$ dB (0.5%). On the other hand, the $SPC-SNR_{PL}$ increases as the acquisition time increases, which results in a decrease in the R_{PL} . An interesting finding is that when the acquisition time is extended to 2s, the $SPC-SNR_{PL}$ increases even above the $SPC-SNR_{EXC}$ value corresponding to this acquisition time. Consequently, the same trend is observed for the R_{PL} and R_{EXC} values at a scanning time of 2 s.

Although it was stated that R_{EXC} and $SPC-SNR_{EXC}$ do not change significantly with the acquisition time, it is worth noting that these values represent only a single PL snapshot at the selected delay $t = 0 \mu s$. The effect of acquisition time is notable for the decay curve reconstruction, which is highly improved both for the noise in I_{EXC} and I_{PL} -- see σ in Fig. 9. Decay deviation σ decreases with the increasing acquisition time. Although both errors are in a different order of magnitude, by increasing the acquisition time from 0.1 s to 2 s, both σ errors decreased by the same ratio.

4.3. Regularization parameter effect

Another way to eliminate the effect of noise is to change the regularization parameter ε in Eq.(2) and Eq.(4). The regularization parameter makes it possible to solve the ill-conditioned problem, where "division by zero" could occur for frequencies with very low amplitude in the I_{EXC} signal [23]. The regularization parameter adds a part of the power of the spectrum to the denominator of the Eq.(2) respective Eq.(4) and thus eliminates the influence of less frequent frequencies in the signal (white noise). As a result, the calculated I_D or I_{DA} is smoothed.

As in the previous section, the influence of the parameter ε was investigated regarding the quality of the reconstructed PL snapshot at the zero delay after excitation, which corresponds to the maximum PL intensity. All simulations were carried with the acquisition time of 0.1 s and a range of ε from 0.05 to 1. Reconstruction parameters and signal properties were held the same as in Section 3. Fig. 10-12 follow the same color scheme as in the previous section with respect to SNR (color) and compression ratio (line/symbol type).

In accordance with the previous results, the effect of the added noise is much more pronounced than the compression ratio used. We will first focus on the influence of regularization parameter ε on the quality of the retrieved image, i.e., R_{EXC} and R_{PL} – see Fig 10. In these results, we see an interplay of two effects: the smoothing of the I_{DA} and I_D , respectively, and the bias of the reconstructed I_{DA} respective I_D . Since the noise level in the I_{EXC} affects the I_{DA} reconstruction less than in I_{PL} , the effect of biased reconstruction of I_{DA} prevails and the R_{EXC} error increase with ε . Whereas in the case of R_{PL} , the noise smoothing effect prevails in I_{DA} for the low ε values and the R_{PL} decreases. However, with increasing ε , the bias effect becomes dominant and the image quality is decreased again.

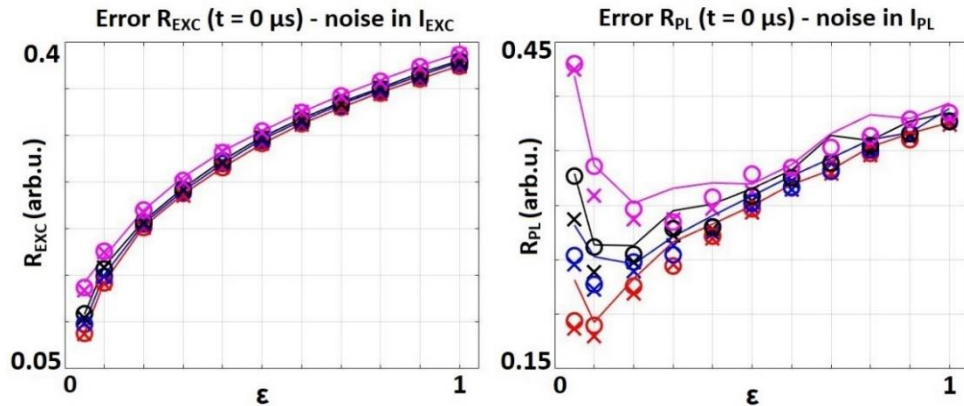


Figure 10: Reconstruction error R_{EXC} (left part), R_{PL} (right part) at the delay $t = 0 \mu\text{s}$ dependence on ϵ - different SNR: 15.2 dB (red), 18.2 dB (blue), 20 dB (black), 23 dB (magenta) and three different compression ratio $k = 0.4$ (full line), $k = 0.6$ (circle), $k = 0.8$ (cross).

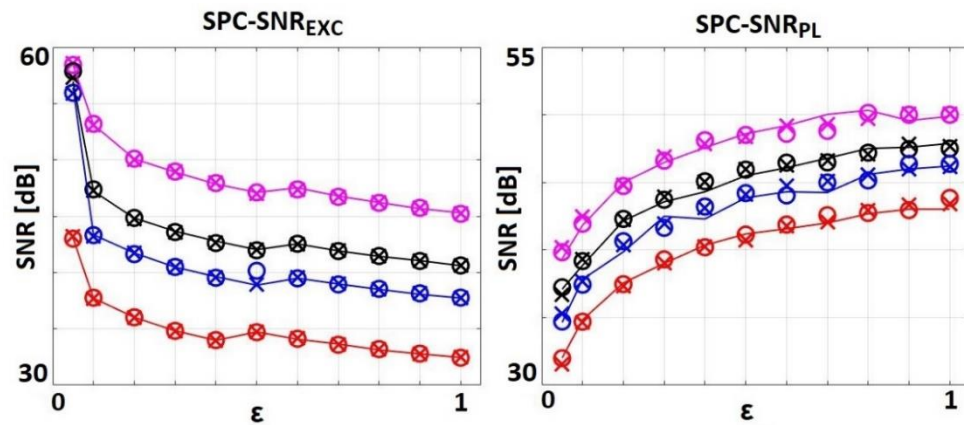


Figure 11: Noise dependence in SPC signal (random fluctuation in intensity of I_D in delay $t = 0 \mu\text{s}$, because of changing illumination masks) on ϵ according to added noise to I_{EXC} (left part) and I_{PL} (right part) with SNR: 15.2 dB (red), 18.2 dB (blue), 20 dB (black), 23 dB (magenta) and three different compression ratio $k = 0.4$ (full line), $k = 0.6$ (circle), $k = 0.8$ (cross).

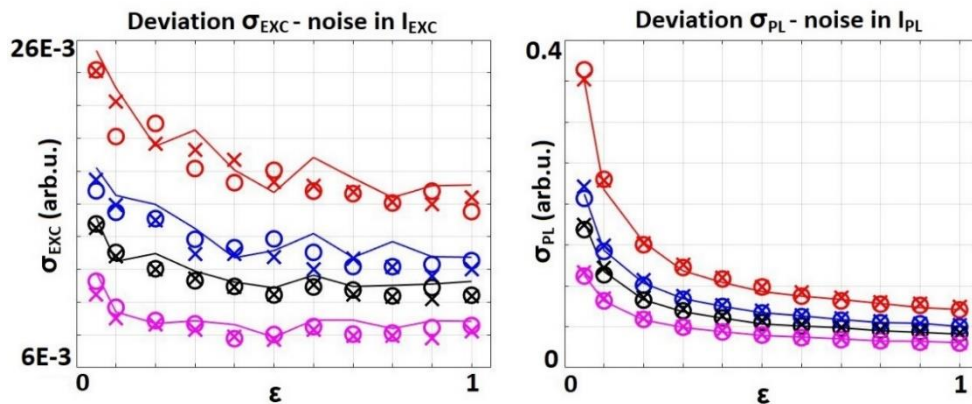


Figure 12: ϵ dependence of σ_{EXC} - noise added to I_{EXC} (left part) and σ_{PL} - noise added to I_{PL} (right part). SNR: 15.2 dB (red), 18.2 dB (blue), 20 dB (black), 23 dB (magenta) and three different compression ratio $k = 0.4$ (full line), $k = 0.6$ (circle), $k = 0.8$ (cross).

This is confirmed by Fig. 11, which shows the amount of noise in the individual $SPC-SNR_{EXC}$ and $SPC-SNR_{PL}$. This implies that for the given noise level in the I_{PL} signal, there is an optimum regularization parameter providing the best results and this provides a guideline of the optimum ε value.

Fig. 12 focuses on σ , which evaluates the fidelity of the reconstructed decay curves. Here, with increasing ε , both σ_{EXC} and σ_{PL} decrease despite the bias effect, i.e., a higher ε value provides a better estimate of the decay curve. We ascribe it to the fact that with decreasing intensity of I_{DA} (the following delay after excitation), the noise level in the SPC signal increases, and thus the smoothing effect of the regularization parameter prevails over the bias effect.

Both the dependence of σ_{EXC} and σ_{PL} on ε are influenced by the amount of noise in the system. Especially for the high-noise PL signal (15.2 dB, 3%), the increase of ε from 0.05 to 1 reduced the σ_{PL} by 79%. Analogously to the previous results, the increase in regularization parameter has a lower effect on the noise introduced via I_{EXC} signal -- see σ_{EXC} , which decreases by 32% for the same noise level and ε change.

5. Conclusion

In this paper, we carried out an extensive analysis of the effect of noise within the RATS technique – a novel method for the PL decay reconstruction and FLIM. Since this is a new method, the findings presented are important for the further direction of the method. The problem was investigated using simulations for cases with noise levels reaching 0.5 -- 3% (SNR 23 -- 15.2dB) of the signal. To disentangle the effect of each noise source, the noise was added to I_{EXC} only and I_{PL} was left noiseless and vice versa.

We consistently observed that the same noise level has a significantly greater effect when present in the I_{PL} , which we ascribe to the fact that the regularization parameter ε is associated with the I_{EXC} in the denominator of the relationship Eq.(2) and Eq.(4). Hence, the most efficient strategy to improve the data quality is to focus on the I_{PL} intensity level and the connected noise.

Secondly, all our data simulations revealed that the effect of noise level is incomparably more important than the compression ratio k , i.e., the number of measured excitation masks in the single-pixel experiment. In other words, for $k > 0.4$, it is not possible to compensate for a higher noise level by increasing the number of excitation masks.

It is also essential to avoid using periodic excitation signals, which can cause periodicity in the retrieved decay and increase the resulting I_D relative noise level. It is worth noting that the RATS method was originally based on an analog random signal generator, the main component of which is a rotary diffuser. Therefore, we attained a quasi-periodic signal, which played a significant role in the method. Using a non-periodic signal, for instance, by laser modulation, a greater signal-to-noise ratio will be obtained.

As expected, we observed that increasing the acquisition time of a single decay measurement (single excitation mask) can highly reduce the resulting noise and effectively compensate for the noise present in the PL measurement. The choice of acquisition time is also connected with the IRF of the signal and the expected PL lifetimes. Moreover, it fundamentally manages total acquisition time. Here we used lifetime $\tau = 20 \mu s$, so that I_{EXC} signal with $IRF = 2.07 \mu s$ was selected with data sampling $0.99 \mu s$. For other signal parameters, different results than those presented here can be achieved after the same signal length extension. If we focus on shorter lifetimes, a faster signal (smaller IRF) is needed, and the total scanning time is also reduced in a given ratio. However, the simulated trends for R , $SPC-SNR$, and σ can be applied without compromising generality.

In order to eliminate signal noise, we have deliberately avoided any mathematical signal filtering techniques so that we do not lose important information due to the random nature of the signal. Mathematical signal filtering could be optimized on the expenses of the general applicability of the results. Therefore, we explored instead the possibility to optimize the regularization parameter ε used in the PL decay retrieval.

The parameter ε was changed in the range 0.05 to 1. We observed a trade-off between the two effects. On the one hand, a higher value of ε smoothes the I_{DA} curve, while, on the other hand, it distorts the I_{DA} because some frequencies of the Fourier spectrum are favored. Therefore, we observed that there is an optimum value of ε connected to the noise level in the I_{PL} signal. As a rule of thumb, for a system with a low noise level, we recommend keeping the parameter ε at 0.1 or 0.2. For a system with a high noise level, it is possible to increase the regularization parameter more significantly.

Funding

Ministry of Education, Youth and Sports ("Partnership for Excellence in Superprecise Optics," Reg. No. CZ.02.1.01/0.0/0.0/16_026/0008390) and the Student Grant Competition at the Technical University of Liberec (under the projects No. SGS-2021-3003).

Acknowledgment

We gratefully acknowledge the Mechanics laboratory of TOPTEC (Institute of Plasma Physics, Czech Academy of Sciences) for providing us with unique optomechanics components since the beginning of RATS method development.

Disclosure

The authors declare no conflicts of interest.

References

1. R. Cubeddu, D. Comelli, C. D'Andrea, P. Taroni, and G. Valentini, "Time-resolved fluorescence imaging in biology and medicine," *J. Phys. D: Appl. Phys.* **35**, R61–R76 (2002).
2. S. Kalinina, J. Breymayer, P. Schäfer, E. Calzia, V. Sheheslavskiy, W. Becker, and A. Rück, "Correlative NAD(P)H-FLIM and oxygen sensing-PLIM for metabolic mapping," *Journal of Biophotonics* **9**, 800–811 (2016).
3. C. D. Wilms, H. Schmidt, and J. Eilers, "Quantitative two-photon Ca²⁺ imaging via fluorescence lifetime analysis," *Cell Calcium* **40**, 73–79 (2006).
4. K. Židek, F. Trojánek, P. Malý, L. Ondič, I. Pelant, K. Dohnalová, L. Šiller, R. Little, and B. R. Horrocks, "Femtosecond luminescence spectroscopy of core states in silicon nanocrystals," *Opt. Express* **18**(24), 25241–25249 (2010).
5. W. Becker, *Advanced Time-Correlated Single Photon Counting Techniques*, Springer, Berlin (2005).
6. J. Sytsma, J. M. Vroom, D. Grauw, and H. C. Gerritsen, "Time-gated fluorescence lifetime imaging and microvolume spectroscopy using two-photon excitation," *J. Microsc.* **191**(1), 39–51 (2008).
7. J. Qu, L. Liu, D. Chen, Z. Lin, G. Xu, B. Guo, and H. Niu, "Temporally and spectrally resolved sampling imaging with a specially designed streak camera," *Opt. Lett.*, **OL 31**, 368–370 (2006).
8. Y. Won, S. Moon, W. Yang, D. Kim, W.-T. Han, and D. Y. Kim, "High-speed confocal fluorescence lifetime imaging microscopy (FLIM) with the analog mean delay (AMD) method," *Opt. Express*, **OE 19**, 3396–3405 (2011).
9. E. Gratton, S. Breusegem, J. D. B. Sutin, Q. Ruan, and N. P. Barry, "Fluorescence lifetime imaging for the two-photon microscope: time-domain and frequency-domain methods," *JBO* **8**, 381–390 (2003).
10. J. Junek, L. Ondič, and K. Židek, "Random temporal laser speckles for the robust measurement of sub-microsecond photoluminescence decay," *Opt. Express*, **OE 28**, 12363–12372 (2020).
11. J. Junek, and K. Židek, "Fluorescence lifetime imaging via spatio-temporal speckle patterns in a single-pixel camera configuration," *Opt. Express*, **OE 29**, 5538–5551 (2021).
12. P. Pande and J. A. Jo, "Automated Analysis of Fluorescence Lifetime Imaging Microscopy (FLIM) Data Based on the Laguerre Deconvolution Method," *IEEE Transactions on Biomedical Engineering* **58**, 172–181 (2011).
13. A. B. Watson, "Probability summation over time," *Vision Research* **19**, 515–522 (1979).
14. T. Regińska, "A Regularization Parameter in Discrete Ill-Posed Problems," *SIAM J. Sci. Comput.* **17**, 740–749 (1996).
15. H. W. Engl, "On the choice of the regularization parameter for iterated Tikhonov regularization of III-posed problems," *Journal of Approximation Theory* **49**, 55–63 (1987).
16. V. Studer, J. Bobin, M. Chahid, H. S. Mousavi, E. Candes, and M. Dahan, "Compressive fluorescence microscopy for biological and hyperspectral imaging," *Proc. Natl. Acad. Sci. U. S. A.* **109**(26), E1679–E1687 (2012).
17. Q. Pian, R. Yao, N. Sinsuebphon, and X. Intes, "Compressive hyperspectral time-resolved wide-field fluorescence lifetime imaging," *Nat. Photonics* **11**(7), 411–414 (2017).
18. K. Židek, O. Denk, and J. Hlubuček, "Lensless Photoluminescence Hyperspectral Camera Employing Random Speckle Patterns," *Sci. Rep.* **7**(1), 15309 (2017).

19. M. F. Duarte, M. A. Davenport, D. Takhar, J. N. Laska, T. Sun, K. F. Kelly, and R. G. Baraniuk, "Single-pixel imaging via compressive sampling," *IEEE Signal Process. Mag.* 25(2), 83–91
20. F. Gascón and F. Salazar, "A simple method to simulate diffraction and speckle patterns with a PC," *Optik* 117(2), 49–57 (2006).
21. C. Li, Wotao Yin, and Yin Zhang, TVAL3 Home, Rice University, 2009, Last updated 11/07/2013, (available from: <https://www.caam.rice.edu/~optimization/L1/TVAL3/>).
22. C. Li, W. Yin, and Y. Zhang, "User's guide for TVAL3: TV minimization by augmented lagrangian and alternating direction algorithms," *CAAM Rep.*20, 46–47 (2009).
23. A. N. Tikhonov and V. Y. Arsenin, "Solutions of ill-posed problems," *SIAM Rev.* 21, 266–267 (1977).